Bio-Design and Manufacturing (2022) 5:617–626
https://doi.org/10.1007/s42242-022-00183-6

PERSPECTIVE

Cell sedimentation during 3D bioprinting: a mini review

Heqi Xu[1] · Jiachen Liu[1] · Zhengyi Zhang[2] · Changxue Xu[1]

Received: 22 September 2021 / Accepted: 5 January 2022 / Published online: 4 February 2022

Graphic abstract

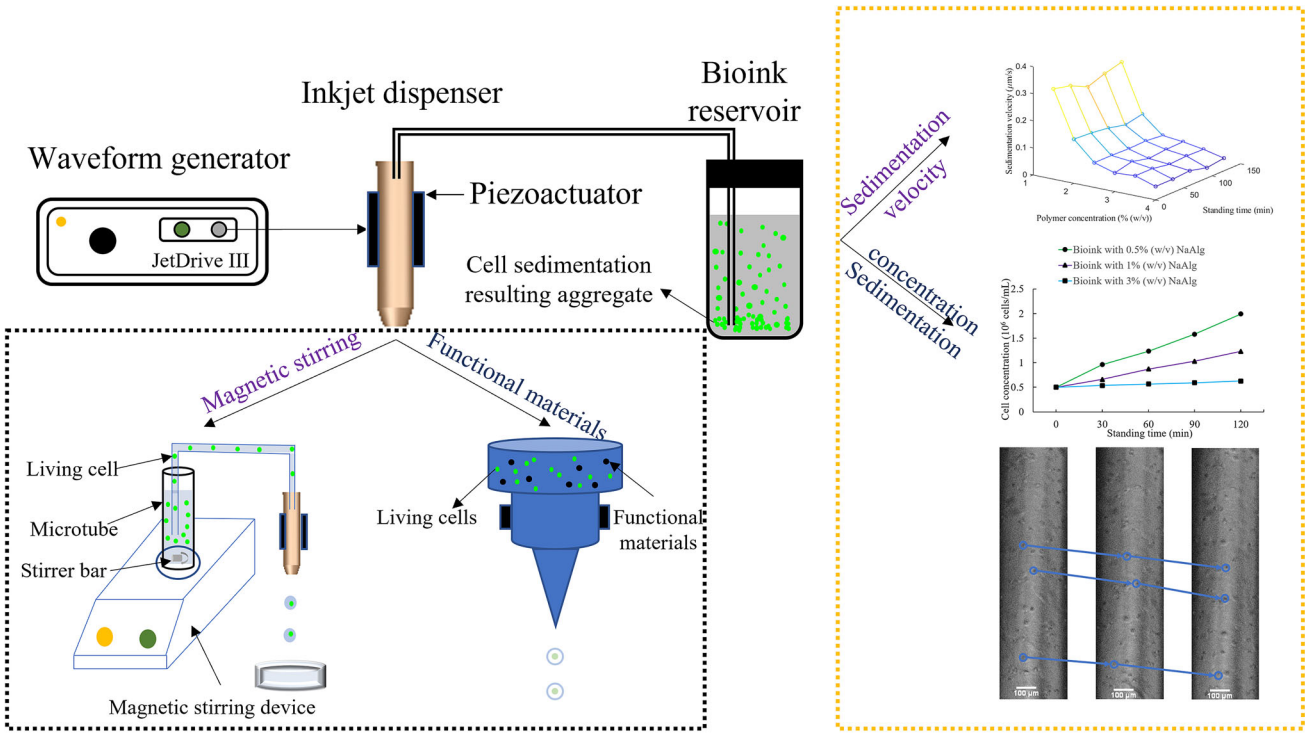

Cell sedimentation mitigation

Cell sedimentation quantification

Introduction

In the past decade, three-dimensional (3D) bioprinting, which precisely deposits bioink composed of the biological materials and the living cells into delicate structures with the living cells encapsulated, has made numerous important advances in tissue engineering and regenerative medicine [1, 2]. Depending on the printing mechanism, 3D bioprinting technologies are generally categorized into four types: inkjet-based bioprinting, microextrusion-based bioprinting, laser-assisted bioprinting, and stereolithography-based bioprinting [3]. Each of these techniques has its benefits and

✉ Zhengyi Zhang
zhengyizhang@hust.edu.cn

✉ Changxue Xu
changxue.xu@ttu.edu

1 Department of Industrial, Manufacturing, and Systems Engineering, Texas Tech University, Lubbock, TX 79409, USA

2 School of Naval Architecture and Ocean Engineering, Huazhong University of Science and Technology, Wuhan 430074, China

drawbacks. For instance, inkjet-based bioprinting has a high printing resolution and good controllability of the deposition of the bioink. However, its tolerance for bioink viscosity is quite limited [4, 5] with only bioinks with the viscosity range of 3–30 mPa·s suitable for this method [6]. Moreover, the cell concentration is limited to the order of 10^6 cells/mL to avoid nozzle clogging and ensure continuous jetting [7]. Meanwhile, microextrusion-based bioprinting, as a low-cost technique, can print bioink with a wide range of viscosities and cell concentrations [8] despite its relatively low post-printing cell viability due to high shear stress [9]. Laser-assisted bioprinting, originating from laser-induced forward transfer (LIFT), can accurately control the resolution of the printed constructs and improve the printing quality. Its disadvantages include high cost and time requirement limiting its wider applications in biomedical engineering [10, 11]. Stereolithography-based bioprinting is capable of fabricating 3D constructs with a high resolution. However, due to the photo-cross-linking mechanism during bioprinting, the material choices for stereolithography are generally restricted to photopolymers [12].

Benefiting from the recent advances in 3D bioprinting techniques and broader choices of biomaterials, 3D bioprinting has been widely performed in a variety of applications including tissue engineering [13, 14], drug screening [15], and regenerative medicine [16]. The biomaterials suitable for 3D bioprinting should bear certain advantages such as shear-thinning properties, good printability, biocompatibility, satisfactory mechanical properties, and easy cross-linking mechanism [17–19]. Naturally derived polymers (such as alginate [20], fibrin [21], and collagen [22]) and synthetic polymers (such as polyethylene glycol (PEG) [23] and gelatin methacrylate (GelMA) [24]) have been widely utilized in 3D bioprinting to mimic the natural extracellular matrix (ECM). A variety of cells (such as NIH/3T3 fibroblasts [25], human mesenchymal stem cells (hMSCs) [26], and human umbilical vein endothelial cells (HUVECs) [27]) have been selected as the model cells for various biomedical applications. Different 3D bioprinting techniques have been implemented to successfully fabricate artificial tissues/organs, such as cartilage [28], skin [29], heart [30], and vascular-like constructs [31], indicating the potential and feasibility to replicate the complex shapes and functions of the 3D native tissues/organs [32]. With the rapid development of technologies and materials, 3D bioprinting is currently envisioned as a promising approach to fabricate 3D functional tissues and organs used for transplantation [33].

3D bioprinting requires a reliable and accurate printing process using cell-laden bioink, which is vital to realize the functionality of printed tissues/organs [34]. Cell sedimentation in the bioink reservoir is a significant challenge during 3D bioprinting, because cell sedimentation facilitates cell aggregation resulting in an unstable printing process and nozzle clogging. Bioink used in 3D bioprinting is a suspension of living cells in a biomaterial solution. Since the gravitational force acting on cells is greater than the buoyant force, the suspended cells in the bioink will sediment with time to the bottom of the bioink reservoir resulting in inhomogeneous cell concentration. The local cell concentration at the reservoir bottom significantly increases, resulting in severe cell adhesion and aggregation. Consequently, the droplet formation process during printing is highly unstable, and cell distribution within the formed microspheres is extremely non-uniform. The overall printing reliability and quality are thus very poor. Notably, cell sedimentation is significant during inkjet-based bioprinting and stereolithography-based bioprinting when low-viscosity bioink is utilized [35]. On the other hand, during microextrusion-based bioprinting and laser-assisted bioprinting, cell sedimentation is usually not significant, because high-viscosity bioink is typically used and cell sedimentation is thus suppressed. However, the bioink used in microextrusion may also have a low viscosity. In that case, cell sedimentation and aggregation become significant due to low viscosity of bioink.

The cell sedimentation phenomenon in the bioink reservoir, as well as its resulting cell aggregation and poor printing reliability and quality during inkjet-based bioprinting, is schematized in Fig. 1. At the beginning of the bioprinting process, the bioink is mixed using a pipette, and the cell spatial distribution within the bioink reservoir is relatively uniform. With the increase in the printing time, the suspended cells sediment to the bioink reservoir bottom, and the local cell concentration at the bottom significantly increases. When the distance between adjacent cells is small enough, the cells adhere to each other to form cell aggregates. These cell aggregates may contain different numbers of cells and their sizes can reach hundreds of micrometers (larger than the nozzle diameter, e.g., 120 μm). Owing to these cell aggregates, the printing process becomes highly unstable and undesirable satellite droplets are formed. Moreover, the cell distribution within the formed microspheres becomes highly non-uniform. Several researchers have reported the negative effects of cell sedimentation on the printing performance during the printing process. For example, Graham et al. studied the effect of cell sedimentation on the cell concentration and reported an increase in cell concentration from the initial $1–1.5 \times 10^7$ cells/mL to 3×10^7 cells/mL [36]. Bhattacharyya et al. reported that the different properties of the bioink at different heights within the bioink reservoir were due to cell sedimentation [37]. Saunders et al. reported poor printing performance due to cell sedimentation after 20-min printing time using inkjet-based bioprinting [38]. The current review is the first of its kind to summarize the phenomena of cell sedimentation, discuss the relevant theories, and explore the strategies to mitigate cell sedimentation during 3D bioprinting. The sections of this paper are

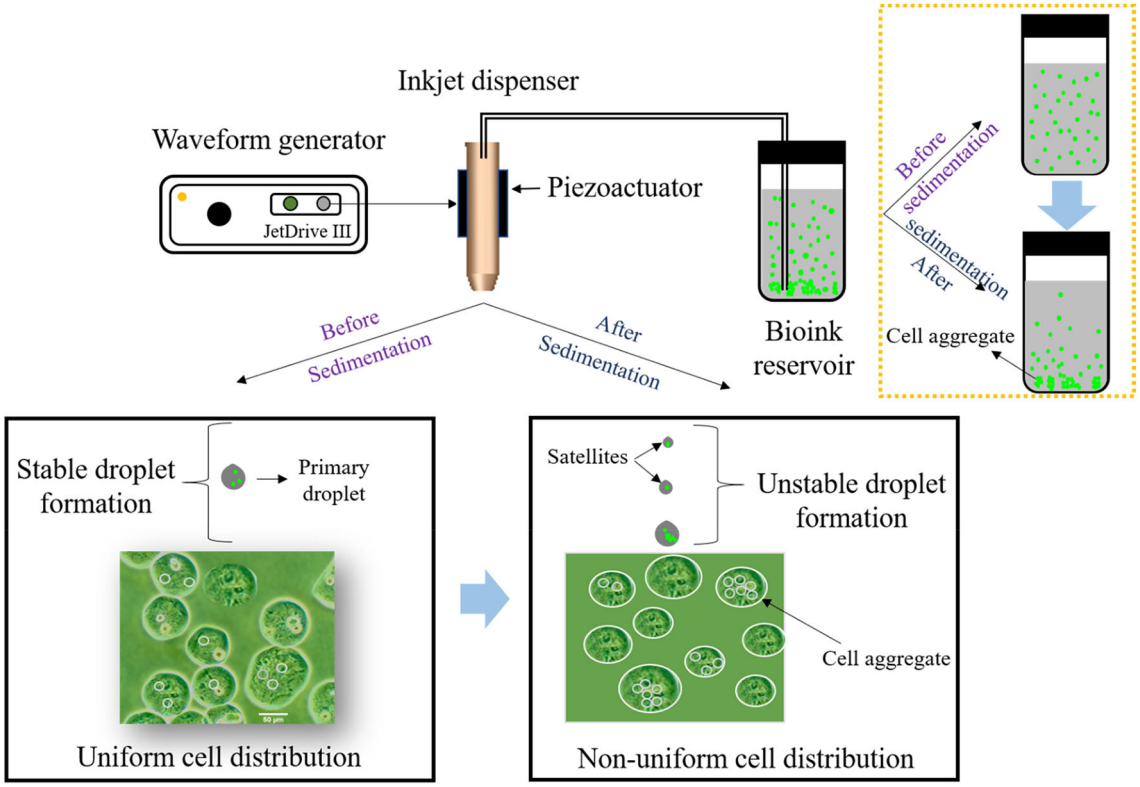

Fig. 1 Consequences of cell sedimentation on the printing quality during inkjet-based bioprinting of bioink containing living cells

organized as follows: The Theory and quantification section summarizes the force analysis during cell sedimentation and the governing equations to quantify osmosis-based mass transfer through the cell membrane; the Mitigation section classifies and discusses different approaches to mitigate the effect of cell sedimentation; the Conclusions and outlook section draws the conclusions based on the current findings and presents some future directions toward better strategies to mitigate cell sedimentation to significantly improve the printing reliability and quality.

Theory and quantification

Theories are important to understand the mechanism of the cell sedimentation phenomenon. Xu et al. systematically studied the cell sedimentation mechanism by conducting a force analysis on a single cell during inkjet-based bioprinting [5]. In general, the cell sedimentation process is determined by four forces including gravitational force, drag force, buoyant force, and force due to cell–cell interaction. The gravitational force can be characterized using the formula

$$G = \rho_c V g \tag{1}$$

where ρ_c represents the cell mass density, V represents the cell volume, and g is the gravitational coefficient. The buoyant force can be estimated using the formula

$$F_b = \rho V g \tag{2}$$

where ρ denotes the fluid density. The drag force can be quantified by the formula

$$F_d = \frac{1}{2}\rho v^2 C_D A \tag{3}$$

where v represents the cell sedimentation velocity, C_D represents the drag coefficient that is related to Reynolds number (Re), and A is the cross-sectional area of a single cell. The adhesion of cells is mediated by the reservable bonds formed between different cells [39], and the force due to cell–cell interaction F_c can be characterized using the bond model

$$F_c = N_b k(x_m - x_\lambda) \tag{4}$$

where N_b represents the bond density, k represents a constant which controls the formation or dissociation of the bonds, and x_m and x_λ are, respectively, the current and the equilibrium lengths of a bond [40, 41]. When a bioink with a low cell concentration is selected for 3D bioprinting, the cells are relatively far away from each other and the force due to cell–cell

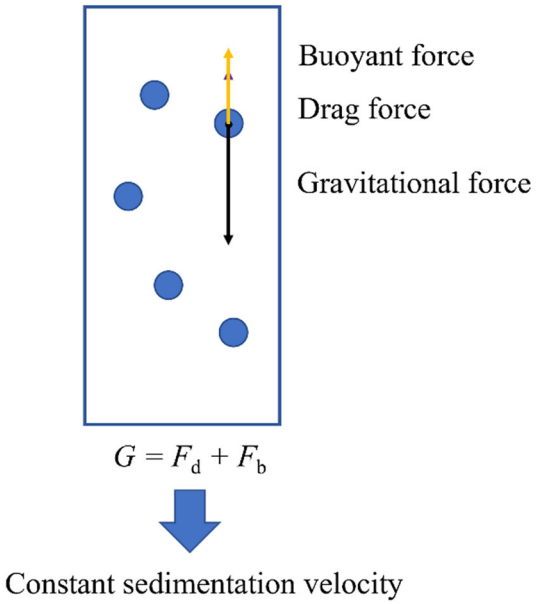

Fig. 2 Force analysis on a single cell during sedimentation when a low cell concentration is selected for 3D bioprinting

interaction is negligible. Since the cell gravitational force is greater than the cell buoyant force, the cells start to sediment and the drag force comes into play. In the steady-state equilibrium, the cell gravitational force is balanced by the cell buoyant force and drag force, as shown in Fig. 2.

With the printing time, cells increasingly sediment to the bottom of the bioink reservoir, resulting in a significant increase in the local cell concentration. The distance between adjacent cells becomes smaller and smaller. When it reaches a critical value (e.g., 4 μm for red blood cells [42]), the force due to cell–cell interaction comes into play; cells start to adhere to each other to form cell aggregates through cell-cell interaction.

Importantly, the cell gravitational force may change during the cell sedimentation process. The cell membrane is selectively permeable. There is water transport due to the osmosis mechanism and ion transport due to the facilitated diffusion mechanism [43, 44]. As shown in Fig. 3, the movement of water into and out of the cells across the permeable membrane occurs through osmosis until equilibrium is reached. This is caused by the concentration gradient of solute inside and outside the cells; water generally moves from a lower solute concentration to a higher solute concentration. Depending on the solute concentration gradient, there are three types of solutions: hypotonic solutions, hypertonic solutions, and isotonic solutions [45]. In hypotonic solutions, the solute concentration is lower than that inside the cells. Water moves into the cells to cause cell swelling, which reduces the cell mass density [46]. In hypertonic solutions, the solute concentration is higher than that inside the cells. Water moves out of the cells to cause cell shrinking, which increases the cell mass density [46]. In isotonic solutions, the solute concentration is equal to that inside the cells. The cells retain their original shape, and cell mass density does not change. However, the size and shape of the cells may change depending on the osmotic water movement [47]. The osmotic pressure is caused by different concentrations of solutes between the two sides of the cell membrane. The magnitude of the osmotic pressure is characterized by the formula

$$\pi = MRT \tag{5}$$

where π represents the osmotic pressure, M represents the molar concentration difference of all solutes on two sides of the membrane, R is the ideal gas constant, and T indicates the absolute temperature. The water diffusion through the cell membrane satisfies Fick's law:

$$J = -\frac{D\Delta C}{\delta} \tag{6}$$

where J denotes the diffusion flux, D is the diffusion coefficient, ΔC represents the solute concentration difference on two sides of the membrane, and δ is the thickness of the membrane. For diffusion of a spherical shape with low Reynolds number, the diffusion coefficient D can be calculated as

$$D = \frac{k_B T}{6\pi \mu r} \tag{7}$$

where k_B denotes Boltzmann's constant, μ represents the dynamic viscosity, and r is the sphere radius. Besides the water transport across the membrane, certain ions (such as K^+, Na^+, and Cl^-) are also selectively permeable to the cell membrane. The ion transport across the cell membrane is realized through facilitated diffusion by specific proteins termed transmembrane proteins present on the membrane surface [48]. The governing equation is

$$\frac{dn}{dt} = -\frac{V_{MAX}}{1 + \frac{K}{dC/d\delta}} \tag{8}$$

where n is the number of ions in the cell, t represents the time, V_{MAX} is the maximum rate of diffusion when all the transmembrane proteins are saturated, and K denotes the concentration gradient of the proteins at the rate of diffusion $0.5V_{MAX}$. Both K and V_{MAX} are physical properties depending on the permeability and surface area of the cells. Finally, with the water diffusion and ion transport across the membrane, the concentration gradient across the cell membrane diminishes and a local concentration equilibrium is achieved.

The cell sedimentation phenomenon has been characterized mainly by measuring the cell sedimentation velocity and

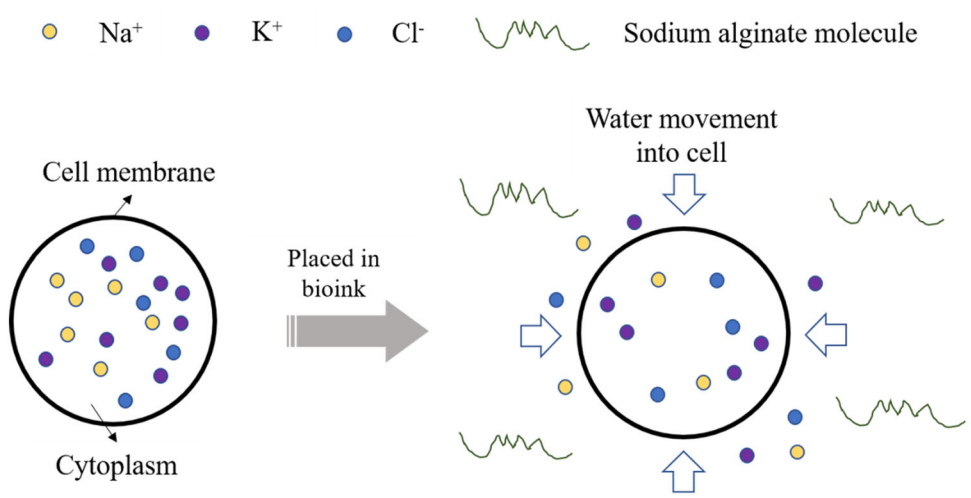

Fig. 3 Water transport due to osmosis mechanism and ion transport due to facilitated diffusion mechanism (Reprinted from [5], Copyright 2019, with permission from The American Institute of Physics)

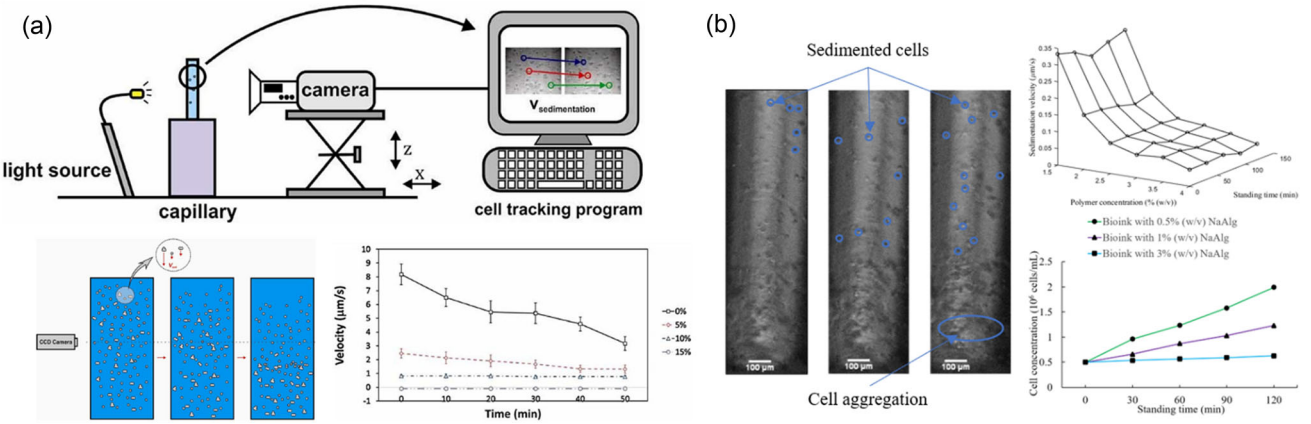

Fig. 4 Cell sedimentation quantification: (a) effect of Ficoll PM400 concentration on the sedimentation velocity of MCF-7 breast cancer cells (Reprinted from [49], Copyright 2012, with permission from Wiley); (b) effects of sodium alginate concentration and printing time on cell sedimentation velocity and the resultant cell concentration at the bottom of the bioink reservoir (Reprinted from [5], Copyright 2019, with permission from The American Institute of Physics)

the resulting cell concentration change. The cell sedimentation velocity is in the order of μm/s. The specific value of cell sedimentation velocity depends on different types of cells with different mass and composition of the bioink (e.g., polymer concentration, biomaterials, etc.). The major findings are displayed in Fig. 4. Chahal et al. utilized a bioink containing MCF-7 breast cancer cells and Ficoll PM400 with different Ficoll concentrations [49]. Without Ficoll PM400, the average cell sedimentation velocity was 7.5 μm/s, which resulted in severe cell sedimentation and clusters of cells. However, this average velocity decreased to 2.3, 0.8, and − 0.15 μm/s when the concentration of Ficoll PM400 increased to 5%, 10%, and 15% (w/v), respectively. This indicated that neutral buoyancy was achieved at 10–15% (w/v) Ficoll PM400. It was observed that larger cell aggregates sedimented faster and a single cell sedimented with a lower velocity. Xu et al. systematically quantified the cell sedimentation velocity and the resultant cell concentration at the bottom of a bioink reservoir using a bioink containing NIH 3T3 mouse fibroblasts and sodium alginate [5]. It was found that the cell sedimentation velocity decreased from 1.45 to 0.65 μm/s when the sodium alginate concentration increased from 0.5% to 1.0% (w/v). The local cell concentration at the bioink reservoir bottom increased with the printing time. Within two hours, the local cell concentration increased by four times from 5×10^5 cells/mL to 2×10^6 cells/mL for the 0.5% (w/v) sodium alginate solution. It was also reported that the cells accumulated at the bioink reservoir bottom and large cell aggregates were observed. Pepper et al. reported a significant change in the uniformity of the bioink due to cell sedimentation during inkjet bioprinting and presented a mathematical model to predict the local cell concentration at the bottom of the bioink reservoir [50]. Both the model and the experimental data showed a linear increase in cell concentration with the printing time as a result of cell sedimentation.

Mitigation

Cell sedimentation results in cell adhesion and aggregation, significantly affecting the bioprinting performance. Various approaches have been proposed to mitigate cell sedimentation, as shown in Fig. 5. These can be mainly classified into two categories: active stirring of the cell-laden bioink and addition of functional biocompatible materials. For the former method, Parsa et al. implemented intermittent stirring in the bioink reservoir using a 3-mm externally actuated magnetic stirrer bar [51]. They found that the sedimentation of Hep G2 hepatoma cells was mitigated, and the reliability of inkjet-based bioprinting process was improved as shown in Fig. 5a. Similarly, Chen et al. applied a magnetic stirring device in the bioink with eight different types of cells (such as 3T3 cells, HepG2, and HUVECs), as shown in Fig. 5b [52]. The results showed that the cell distribution within the bioink was almost homogeneous, and the formed droplets with one single cell were improved by 43.8%. Other researchers utilized neutral buoyancy to mitigate cell sedimentation. The polymer concentration was elevated to increase the buoyant force until the cell gravitational force was balanced. Parsa et al. also added the biocompatible surfactant Pluronic with 0.05% concentration into the bioink containing Hep G2 hepatocytes [51]. It was found that the cell viability remained above 95% after two-day incubation. Chahal et al. added Ficoll PM400 into the bioink containing MCF-7 breast cancer cells to mitigate cell sedimentation, as shown in Fig. 5c [49]. It was found that the neutral buoyancy occurred between 10 and 15% Ficoll PM400, and the cell viability was not affected. The experimental results also demonstrated that, through the addition of Ficoll PM400, the chance of nozzle clogging was significantly reduced, and the cell distribution after the piezoelectric inkjet printing process became more consistent. Ng et al. incorporated different concentrations of polyvinylpyrrolidone (PVP) macromolecules in the bioink to mitigate cell sedimentation during the drop-on-demand microvalve-based bioprinting process, as shown in Fig. 5d [53]. The addition of PVP macromolecules up to 3% (w/v) proved to significantly mitigate cell sedimentation and improve the printing consistency. Na et al. mixed biocompatible silk fibroin (SF) particles within GelMA-based bioink containing NIH 3T3 cells in projection-based stereolithography, as shown in Fig. 5e [54]. It was found that the addition of up to 1% SF particles improved the uniformity of cells in each layer, and the cells maintained good metabolic activity. Lindsay et al. added a small amount of calcium cations to the alginate-based bioink containing neural progenitor cells in microextrusion bioprinting [55]. The alginate-based bioink was lightly cross-linked to form a weak gel during first-stage cross-linking, which effectively prevented cell sedimentation. Then, a follow-up second-stage cross-linking was performed by using a larger volume of calcium after the printing process.

Although the aforementioned approaches have proved as effective to mitigate cell sedimentation, some important concerns remain. Parsa et al. reported that the cell viability was significantly decreased from 100% to around 75% within 50-min stirring time, indicating the cell damage during the stirring process [51]. Moreover, the addition of functional particles and biomaterials may increase the viscosity of the cell-laden bioink, which may affect wide applications of the bioink in inkjet-based and stereolithography-based bioprinting. The selections of the functional particles and biomaterials are also limited. Finally, some of the approaches may not be applicable for bioink with multiple cell types, because different cells have different mass densities. For example, the mass density of mouse lymphocytic leukemia cells (L1210) is in the range of 1.05–1.12 g/mL [56]; that of human lung carcinoma cells (H1650) is in the range of 1.04–1.06 g/mL [57]; and that of yeast cells is in the range of 1.1–1.11 g/mL [58]. Active stirring implements magnetic stirrer bars to consistently mix the cell-laden bioink. This approach is mechanical mixing-based and is applicable for bioink containing different types of cells. However, mechanical mixing may result in cell damage, especially for some types of cells that are sensitive to mechanical stresses. Other approaches to mitigate cell sedimentation comprise adding functional materials to reduce the difference between the cell mass density and the bioink mass density. It is known that different types of cells have different cell mass densities. For different types of cells, the bioink should be carefully formulated. Moreover, it is extremely difficult to accommodate multiple cell types in the bioink to achieve neutral buoyancy. In summary, cell sedimentation is a significant challenge in 3D bioprinting, playing a pivotal role in cell aggregation as well as the overall printing reliability and quality. Therefore, it is critical to investigate new effective and efficient mitigation approaches.

Conclusions and outlook

This review, as the first of its kind specifically focusing on the cell sedimentation phenomenon in 3D bioprinting, helps to draw more attention to this phenomenon and its effects on printing reliability and quality. The summary of this mini review is provided in Table 1. During cell culture, cells may have different attachment levels exhibiting different aspect ratios depending on the culture conditions, which further affects cell gravity, as well as the corresponding cell sedimentation during the bioprinting process. The bioink used for 3D bioprinting contains suspended living cells. With the printing time, the suspended cells sediment to the bottom of the bioink reservoir, which is recognized as an important

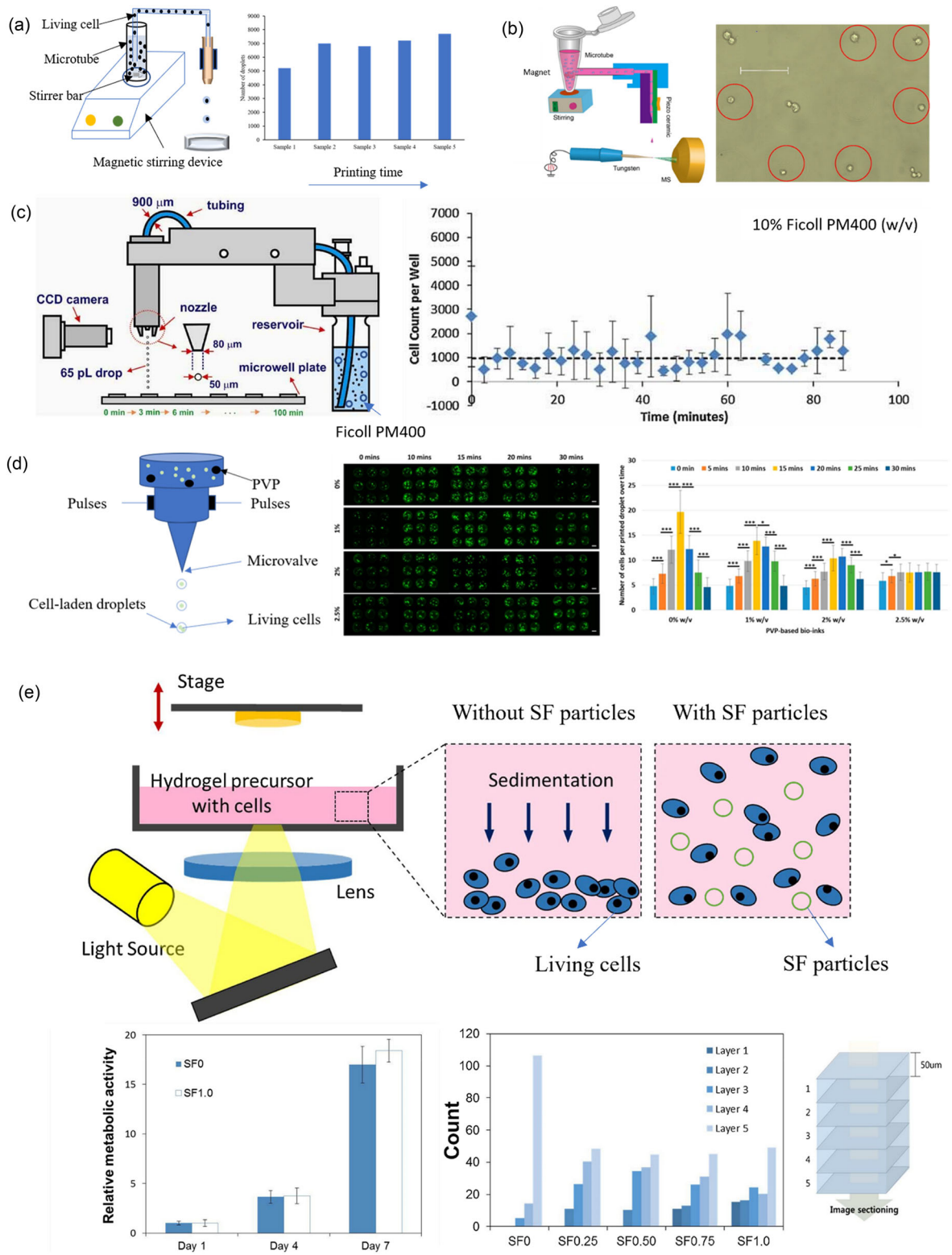

Fig. 5 Approaches to mitigate cell sedimentation: (a) intermittent stirring using a magnetic stirrer bar in inkjet bioprinting; (b) utilizing a magnetic stirring device in inkjet bioprinting (Reprinted from [52], Copyright 2016, with permission from American Chemical Society); (c) addition of Ficoll PM400 to achieve neutral buoyancy in inkjet bioprinting (Reprinted from [49], Copyright 2012, with permission from Wiley); (d) addition of PVP macromolecules in microvalve-based bioprinting (Reprinted from [53], Copyright 2017, with permission from MDPI); (e) addition of SF particles to increase the viscosity of the bioink in projection-based stereolithography (Reprinted from [54], Copyright 2018, with permission from Elsevier)

Table 1 Summary of this mini review

Consequence	Reduced printing reliability	Non-uniform cell distribution [37, 49] Cell aggregation [5, 49, 50]
Theory	Force analysis	Force equilibrium [5]
	Osmosis-based mass transfer	Mass transfer [46–48]
Quantification	Sedimentation-related parameters	Cell sedimentation velocity [5, 49]
		Cell concentration [5, 36]
Mitigation	Active stirring	Magnetic stirring [51, 52]
	Functional biocompatible materials	Ficoll PM400 [49]
		PVP macromolecules [53]
		SF particles [54]

challenge in 3D bioprinting, as it is directly related to cell adhesion and aggregation, significantly affecting the printing performance during 3D bioprinting. The cell sedimentation phenomenon is governed by four forces, including gravitational force, buoyant force, drag force, and force due to cell–cell interaction. The mass density of cells may change through water transport due to osmosis and ion transport due to facilitated diffusion mechanism. The physics-based model proposed in this study helps to tackle the complex dynamics in cell sedimentation. However, there are some significant challenges to fully understand this complex process, including the precise quantification of cell gravity and mass transfer through the cell membrane. Several research groups have measured the cell sedimentation velocity and investigated the effects of polymer concentration and printing time on cell sedimentation velocity and local cell concentration at the bottom of the bioink reservoir. Some approaches have targeted the mitigation of cell sedimentation, which can be mainly classified into two categories: active stirring of the cell-laden bioink and addition of functional biocompatible materials. Although the proposed approaches proved as effective, there are some important concerns including decreased cell viability, limited selection of the functional materials, and inability to accommodate multiple cell types. In addition to bioink concentration and viscosity, there are other parameters that may affect cell sedimentation and aggregation in 3D bioprinting, such as the binding between biochemical ligands and the receptors on the cell membrane. Hence, it is critical to investigate new effective and efficient mitigation approaches. The future directions comprise the utilization of functional nanoparticles attached to cell membranes to enable the manipulation of cell motions through electric fields or magnetic fields [59, 60]. Cell sedimentation is a multidisciplinary topic involving material sciences, mechanical engineering, and biomedical engineering. Approaches integrating these fields to mitigate cell sedimentation should be developed to ensure printing reliability and quality as well as the functionality of the fabricated tissues and organs using 3D bioprinting.

Author contributions HX was involved in writing the original draft, conceptualization, and formal analysis; JL helped in writing, review, and editing; ZZ and CX helped in conceptualization, and writing, review, and editing.

Declarations

Conflict of interest The authors declare that there is no conflict of interest.

Ethical approval This study does not contain any studies with human or animal subjects performed by any of the authors.

References

1. Derakhshanfar S, Mbeleck R, Xu K et al (2018) 3D bioprinting for biomedical devices and tissue engineering: a review of recent trends and advances. Bioact Mater 3:144–156. https://doi.org/10.1016/j.bioactmat.2017.11.008
2. Holland I, Logan J, Shi J et al (2018) 3D biofabrication for tubular tissue engineering. Bio-des Manuf 1:89–100. https://doi.org/10.1007/s42242-018-0013-2
3. Foyt DA, Norman MD, Yu TT et al (2018) Exploiting advanced hydrogel technologies to address key challenges in regenerative medicine. Adv Healthc Mater 7:1700939. https://doi.org/10.1002/adhm.201700939
4. Xu H, Casillas J, Xu C (2019) Effects of printing conditions on cell distribution within microspheres during inkjet-based bioprinting. AIP Adv 9:095055. https://doi.org/10.1063/1.5116371
5. Xu H, Zhang Z, Xu C (2019) Sedimentation study of bioink containing living cells. J Appl Phys 125:114901. https://doi.org/10.1063/1.5089245
6. Saunders RE, Derby B (2014) Inkjet printing biomaterials for tissue engineering: bioprinting. Int Mater Rev 59:430–448. https://doi.org/10.1179/1743280414Y.0000000040
7. Nakamura M, Kobayashi A, Takagi F et al (2005) Biocompatible inkjet printing technique for designed seeding of individual living cells. Tissue Eng 11:1658–1666. https://doi.org/10.1089/ten.2005.11.1658
8. Jones N (2012) Science in three dimensions: the print revolution. Nature 487:22. https://doi.org/10.1038/487022a
9. Chang R, Nam J, Sun W (2008) Effects of dispensing pressure and nozzle diameter on cell survival from solid freeform fabrication-based direct cell writing. Tissue Eng Part A 14:41–48. https://doi.org/10.1089/ten.a.2007.0004

10. Huang Y, Zhang XF, Gao G et al (2017) 3D bioprinting and the current applications in tissue engineering. Biotechnol J 12:1600734. https://doi.org/10.1002/biot.201600734
11. Mandrycky C, Wang Z, Kim K et al (2016) 3D bioprinting for engineering complex tissues. Biotechnol Adv 34:422–434. https://doi.org/10.1016/j.biotechadv.2015.12.011
12. Chia HN, Wu BM (2015) Recent advances in 3D printing of biomaterials. J Biol Eng 9:1–14. https://doi.org/10.1186/s13036-015-0001-4
13. Duan B (2017) State-of-the-art review of 3D bioprinting for cardiovascular tissue engineering. Ann Biomed Eng 45:195–209. https://doi.org/10.1007/s10439-016-1607-5
14. Yin J, Zhao D, Liu J (2019) Trends on physical understanding of bioink printability. Bio-des Manuf 2:50–54. https://doi.org/10.1007/s42242-019-00033-y
15. Nie J, Gao Q, Fu J et al (2020) Grafting of 3D bioprinting to in vitro drug screening: a review. Adv Healthc Mater 9:1901773. https://doi.org/10.1002/adhm.201901773
16. Murphy SV, Atala A (2014) 3D bioprinting of tissues and organs. Nat Biotechnol 32:773. https://doi.org/10.1038/nbt.2958
17. Gungor-Ozkerim PS, Inci I, Zhang YS et al (2018) Bioinks for 3D bioprinting: an overview. Biomater Sci 6:915–946. https://doi.org/10.1039/c7bm00765e
18. Boularaoui S, Al Hussein G, Khan KA et al (2020) An overview of extrusion-based bioprinting with a focus on induced shear stress and its effect on cell viability. Bioprinting 20:e00093. https://doi.org/10.1016/j.bprint.2020.e00093
19. Zhang B, Luo Y, Ma L et al (2018) 3D bioprinting: an emerging technology full of opportunities and challenges. Bio-des Manuf 1:2–13. https://doi.org/10.1007/s42242-018-0004-3
20. Xu C, Zhang Z, Christensen K et al (2014) Freeform vertical and horizontal fabrication of alginate-based vascular-like tubular constructs using inkjetting. J Manuf Sci Eng 136:061020. https://doi.org/10.1115/1.4028578
21. De Melo BA, Jodat YA, Cruz EM et al (2020) Strategies to use fibrinogen as bioink for 3D bioprinting fibrin-based soft and hard tissues. Acta Biomater 117:60–76. https://doi.org/10.1016/j.actbio.2020.09.024
22. Lee A, Hudson A, Shiwarski D et al (2019) 3D bioprinting of collagen to rebuild components of the human heart. Science 365:482–487. https://doi.org/10.1126/science.aav9051
23. Xin S, Chimene D, Garza JE et al (2019) Clickable PEG hydrogel microspheres as building blocks for 3D bioprinting. Biomater Sci 7:1179–1187. https://doi.org/10.1039/c8bm01286e
24. Yin J, Yan M, Wang Y et al (2018) 3D bioprinting of low-concentration cell-laden gelatin methacrylate (GelMA) bioinks with a two-step cross-linking strategy. ACS Appl Mater Interf 10:6849–6857. https://doi.org/10.1021/acsami.7b16059
25. Wang Z, Abdulla R, Parker B et al (2015) A simple and high-resolution stereolithography-based 3D bioprinting system using visible light crosslinkable bioinks. Biofabrication 7:045009. https://doi.org/10.1088/1758-5090/7/4/045009
26. Gaebel R, Ma N, Liu J et al (2011) Patterning human stem cells and endothelial cells with laser printing for cardiac regeneration. Biomaterials 32:9218–9230. https://doi.org/10.1016/j.biomaterials.2011.08.071
27. Zhang YS, Arneri A, Bersini S et al (2016) Bioprinting 3D microfibrous scaffolds for engineering endothelialized myocardium and heart-on-a-chip. Biomaterials 110:45–59. https://doi.org/10.1016/j.biomaterials.2016.09.003
28. Abbadessa A, Mouser VH, Blokzijl MM et al (2016) A synthetic thermosensitive hydrogel for cartilage bioprinting and its biofunctionalization with polysaccharides. Biomacromol 17:2137–2147. https://doi.org/10.1021/acs.biomac.6b00366
29. Cubo N, Garcia M, Del Cañizo JF et al (2016) 3D bioprinting of functional human skin: production and in vivo analysis. Biofabrication 9:015006. https://doi.org/10.1088/1758-5090/9/1/015006
30. Mirdamadi E, Tashman JW, Shiwarski DJ et al (2020) Fresh 3D bioprinting a full-size model of the human heart. ACS Biomater Sci Eng 6:6453–6459. https://doi.org/10.1021/acsbiomaterials.0c01133
31. Xu H, Casillas J, Krishnamoorthy S et al (2020) Effect of Irgacure 2959 and lithium phenyl-2, 4, 6-trimethylbenzoylphosphinate on cell viability, physical properties, and microstructure in 3D bioprinting of vascular-like constructs. Biomed Mater 15:055021. https://doi.org/10.1088/1748-605X/ab954e
32. Ribeiro A, Blokzijl MM, Levato R et al (2017) Assessing bioink shape fidelity to aid material development in 3D bioprinting. Biofabrication 10:014102. https://doi.org/10.1088/1758-5090/aa90e2
33. Jian H, Wang M, Wang S et al (2018) 3D bioprinting for cell culture and tissue fabrication. Bio-des Manuf 1:45–61. https://doi.org/10.1007/s42242-018-0006-1
34. Griffith LG, Swartz MA (2006) Capturing complex 3D tissue physiology in vitro. Nat Rev Mol Cell Bio 7:211–224. https://doi.org/10.1038/nrm1858
35. Liu F, Liu C, Chen Q, et al (2018) Progress in organ 3D bioprinting. Int J Bioprint 4:128. https://doi.org/10.18063/IJB.v4i1.128
36. Graham AD, Olof SN, Burke MJ et al (2017) High-resolution patterned cellular constructs by droplet-based 3D printing. Sci Rep 7:1–11. https://doi.org/10.1038/s41598-017-06358-x
37. Bhattacharyya A, Janarthanan G, Tran HN et al (2021) Bioink homogeneity control during 3D bioprinting of multicomponent micro/nanocomposite hydrogel for even tissue regeneration using novel twin screw extrusion system. Chem Eng J 415:128971. https://doi.org/10.1016/j.cej.2021.128971
38. Saunders RE, Gough JE, Derby B (2008) Delivery of human fibroblast cells by piezoelectric drop-on-demand inkjet printing. Biomaterials 29:193–203. https://doi.org/10.1016/j.biomaterials.2007.09.032
39. Bell GI (1978) Models for the specific adhesion of cells to cells. Science 200:618–627. https://doi.org/10.1126/science.347575
40. N'dri N, Shyy W, Tran-Son-Tay R, (2003) Computational modeling of cell adhesion and movement using a continuum-kinetics approach. Biophys J 85:2273–2286. https://doi.org/10.1016/S0006-3495(03)74652-9
41. Dembo M, Torney D, Saxman K, et al (1988) The reaction-limited kinetics of membrane-to-surface adhesion and detachment. Proc Royal Soc B P Roy Soc B Biol Sci 234:55–83. https://doi.org/10.1098/rspb.1988.0038
42. Kim S, Popel AS, Intaglietta M et al (2005) Aggregate formation of erythrocytes in postcapillary venules. Am J Physiol Heart Circ 288:H584–H590. https://doi.org/10.1152/ajpheart.00690.2004
43. Goodhead LK, MacMillan FM (2017) Measuring osmosis and hemolysis of red blood cells. Adv Physiol Educ 41:298–305. https://doi.org/10.1152/advan.00083.2016
44. Kimizuka H, Koketsu K (1964) Ion transport through cell membrane. J Theor Biol 6:290–305. https://doi.org/10.1016/0022-5193(64)90035-9
45. Vujovic P, Chirillo M, Silverthorn DU (2018) Learning (by) osmosis: an approach to teaching osmolarity and tonicity. Adv Physiol Edu 42:626–635. https://doi.org/10.1152/advan.00094.2018
46. Baldwin WW, Sheu M, Bankston P et al (1988) Changes in buoyant density and cell size of Escherichia coli in response to osmotic shocks. J Bacteriol 170:452–455. https://doi.org/10.1128/jb.170.1.452-455.1988
47. Strange K (2004) Cellular volume homeostasis Adv Physiol Edu 28:155–159. https://doi.org/10.1152/advan.00034.2004

48. Hammar P, Leroy P, Mahmutovic A et al (2012) The *lac* repressor displays facilitated diffusion in living cells. Science 336:1595–1598. https://doi.org/10.1126/science.1221648
49. Chahal D, Ahmadi A, Cheung KC (2012) Improving piezoelectric cell printing accuracy and reliability through neutral buoyancy of suspensions. Biotechnol Bioeng 109:2932–2940. https://doi.org/10.1002/bit.24562
50. Pepper ME, Seshadri V, Burg TC et al (2012) Characterizing the effects of cell settling on bioprinter output. Biofabrication 4:011001. https://doi.org/10.1088/1758-5082/4/1/011001
51. Parsa S, Gupta M, Loizeau F et al (2010) Effects of surfactant and gentle agitation on inkjet dispensing of living cells. Biofabrication 2:025003. https://doi.org/10.1088/1758-5082/2/2/025003
52. Chen F, Lin L, Zhang J et al (2016) Single-cell analysis using drop-on-demand inkjet printing and probe electrospray ionization mass spectrometry. Anal Chem 88:4354–4360. https://doi.org/10.1021/acs.analchem.5b04749
53. Ng WL, Yeong WY, Naing MW (2017) Polyvinylpyrrolidone-based bio-ink improves cell viability and homogeneity during drop-on-demand printing. Materials 10:190. https://doi.org/10.3390/ma10020190
54. Na K, Shin S, Lee H et al (2018) Effect of solution viscosity on retardation of cell sedimentation in DLP 3D printing of gelatin methacrylate/silk fibroin bioink. J Ind Eng Chem 61:340–347. https://doi.org/10.1016/j.jiec.2017.12.032
55. Lindsay CD, Roth JG, LeSavage BL et al (2019) Bioprinting of stem cell expansion lattices. Acta Biomater 95:225–235. https://doi.org/10.1016/j.actbio.2019.05.014
56. Zhao Y, Lai HSS, Zhang G et al (2015) Measurement of single leukemia cell's density and mass using optically induced electric field in a microfluidics chip. Biomicrofluidics 9:022406. https://doi.org/10.1063/1.4917290
57. Bryan AK, Hecht VC, ShenW, et al (2014) Measuring single cell mass, volume, and density with dual suspended microchannel resonators. Lab Chip 14:569–576. https://doi.org/10.1039/c3lc51022k
58. Bryan AK, Goranov A, Amon A et al (2010) Measurement of mass, density, and volume during the cell cycle of yeast. PNAS 107:999–1004. https://doi.org/10.1073/pnas.0901851107
59. Gertz F, Khitun A (2016) Biological cell manipulation by magnetic nanoparticles. AIP Adv 6:025308. https://doi.org/10.1063/1.4942090
60. Arocena M, Zhao M, Collinson JM et al (2010) A time-lapse and quantitative modelling analysis of neural stem cell motion in the absence of directional cues and in electric fields. J Neurosci Res 88:3267–3274. https://doi.org/10.1002/jnr.22502